

Imaging of dislocation bundles by micro-Raman line width mapping to assess the structural quality of heteroepitaxial diamond for detector applications*

M. Mayr¹, M. Fischer¹, S. Gsell¹, C. Stehl¹, M. Schreck^{1,‡}, and E. Berdermann² for the ADAMAS collaboration

¹Universität Augsburg, Augsburg, Germany; ²GSI, Darmstadt, Germany

Within the ADAMAS collaboration, the role of the diamond group at the University of Augsburg is to develop and manufacture large-area high-quality single crystal diamond suitable for the construction of detectors for heavy ions and minimum ionising particles. In contrast to current samples grown by homoepitaxy on substrates with maximum lateral dimensions of ~10 mm, the heteroepitaxial deposition is done on the Ir/YSZ/Si(001) multilayer system that is available in 100 mm wafer size. As a consequence, these samples that are often known as “Diamond on Iridium” (DoI) offer a realistic chance for a scaling to large areas as required for tracking applications.

Major challenges, however, are the occurrence of polarization effects and an incomplete charge collection with charge collection efficiencies (CCE) varying from sample to sample. These effects are mainly attributed to properties of the bulk, namely lattice defects like dislocations and point defects, generating both deep and shallow charge carrier traps. Being able to control and further reduce the density of these defects is compulsory for future application of DoI material not only in particle physics.

Imaging and quantification of dislocations

A controlled optimization of material synthesis requires efficient concepts for a visualization and quantitative evaluation of threading dislocations. A standard technique for the assessment of dislocation densities uses preferential etching with subsequent counting of the etch-pits. Furthermore, inside the bulk dislocations create inhomogeneous strain fields which broaden XRD- and Raman line profiles. We recently revealed that the density of dislocations as derived from etching experiments shows a characteristic correlation with film thickness [1] and with the width of the diamond Raman line (see Fig. 1).

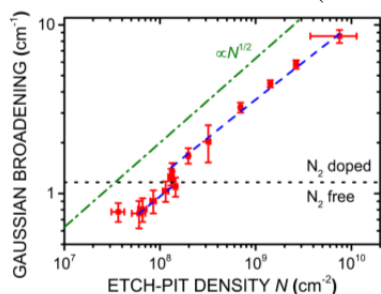


Figure 1: Broadening of the Raman peak vs. etch-pit density. The continuous variation of the dislocation density was achieved by growth of a thick film. The blue fit curve uses the relationship given by Eq. (1). The displaced green curve describes a simple \sqrt{N} behaviour. [1]

* Work supported by EU (HadronPhysics3 project No. 283286) and GSI (Platform for Detectors and Systems).

[‡]matthias.schreck@physik.uni-augsburg.de

The relationship between the mean square strain and the dislocation density N (in cm^{-2}) is described by (1):

$$\overline{\varepsilon_N^2} \propto N \cdot \ln \frac{10^7}{2 \cdot \sqrt{N}} \quad (1)$$

Using this approach, it is possible to image the spatial distribution of dislocations by mapping the Raman line width. The stripe pattern in the cross section map (see Fig. 2) is interpreted in terms of bundles of threading dislocations which are tilted away from the surface normal by several degrees. Tilting is attributed to lateral step flow during growth on off-axis substrates [2]. Understanding the interaction between dislocations and surface features is important for a further reduction of defect densities.

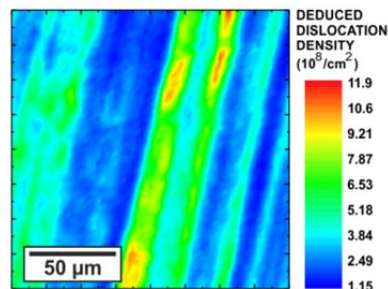


Figure 2: Cross-sectional dislocation density map of a DoI sample grown with 100 ppm N_2 on a (001) substrate with [100] off-axis direction, as derived from high-resolution Raman-line width measurements using the calibration curve in Fig. 1.

DoI: state of the art

In the meantime, continuous improvement in heteroepitaxial diamond growth and post-processing (lapping, polishing) has yielded DoI samples with lateral dimensions up to $2 \times 2 \text{ cm}^2$ (see Fig. 3) and thin membranes down a thickness of $80 \mu\text{m}$. For further thinning and also removing of polishing defects, reactive ion etching (RIE) was successfully applied.

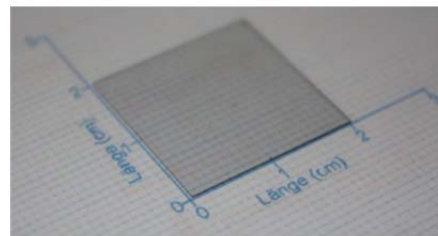


Figure 3: $2 \times 2 \text{ cm}^2$ DoI sample supplied to GSI for measurements of the detector properties.

References

- [1] C. Stehl et al., Appl. Phys. Lett. **103**, 2013.
- [2] M. Mayr et al., Phys. Status Solidi A **211**, 2014.